Journal of Catalysis 260 (2008) 75–80

Contents lists available at ScienceDirect

Journal of Catalysis

www.elsevier.com/locate/jcat

The effect of surface OH-population on the photocatalytic activity of rare earth-doped P25-TiO_2 in methylene blue degradation

P. Du, A. Bueno-López, M. Verbaas, A.R. Almeida, M. Makkee, J.A. Moulijn, G. Mul *

Catalysis Engineering, DelftChemTech, Delft University of Technology, Julianalaan 136, 2628 BL Delft, The Netherlands

ARTICLE INFO

Article history:
Received 20 February 2008
Revised 2 September 2008
Accepted 3 September 2008
Available online 1 October 2008

Keywords:
Photocatalysis
Rare earth
TiO_2
Doping
Methylene blue
Surface OH-groups
Infrared
Fluorescence
Combinatorial photoreactor

ABSTRACT

Commercial TiO_2 (P25, from Degussa) was modified with variable amounts of La, Ce, Y, Pr, Sm (generally rare earth (RE)), by thermal treatment of physical mixtures of TiO_2 and the nitrates of the various RE. Doping of P25 with RE, combined with calcination at 600 or 800 °C, yields materials with surface areas ranging from ~10 to 50 m^2/g, and an anatase to rutile phase ratio ranging from ~0.03 to 0.7, as determined by evaluation of XRD data. After calcination at 600 °C, unpromoted P25 yields the highest activity in methylene blue degradation, while RE addition decreases the activity. After pretreatment of P25 at 800 °C, RE modified catalysts perform better than unpromoted P-25, La being the preferred RE. By evaluation of the DRIFT spectra of the various catalysts, a correlation between the number of a specific anatase Ti–OH group, yielding an IR absorption at 3635 cm^{-1}, and the methylene blue degradation rate was determined. This suggests that this OH-group is an important precursor for the reactive site in aqueous phase methylene blue degradation, and a dominant factor in controlling performance of P-25 in this reaction.

1. Introduction

Over the last decades, TiO_2 based materials have been intensively studied as photocatalysts [1–4]. To enhance the quantum yield of commercially available TiO_2, which is typically below 1%, TiO_2 particles have often been chemically modified. While many reports exist on modification with transition metal oxides to enhance the quantum yield and visible light sensitivity, the effect of doping with lanthanides has been less extensively investigated. Generally a positive effect of La-doping on photocatalytic activity of TiO_2 is reported. Inhibition of recombination of electrons and holes [5–7], or beneficial surface adsorption properties [8–10] have been proposed to explain this positive effect. Both explanations are based on a direct involvement of the promoter in the reactions, which include methylene blue degradation [5], nitrite degradation [6], 2-mercaptobenzothiazole decomposition [7], rhodamine B degradation [8], and salicylic, *t*-cinnamic acid, and *p*-chlorophenoxyacetic acid degradation [9,10].

The main objective of the present study is to further evaluate the photocatalytic performance of a commercial TiO_2 photocatalyst P25 from Degussa after modification with rare earth oxides (La, Ce, Y, Pr, and Sm) in the methylene blue decomposition reaction at 370 nm. We compared performance after calcination at 600 or 800 °C, representative of pretreatment conditions applied in other studies [5–10]. Furthermore we specifically tried to correlate the degradation rate to material properties, i.e. the surface area, anatase/rutile ratio of the samples, and the nature of the hydroxyl groups present on the catalyst surface as determined by diffuse reflectance infrared spectroscopy. From the extensive data set it can be derived that the number of specific surface anatase–OH groups available in the light exposed reactor volume shows a strong correlation with the observed methylene blue decomposition rate, suggesting that these groups are largely determining the P-25 reactivity for this specific reaction.

2. Experimental

2.1. Photocatalyst preparation

Rare earth (RE)-doped TiO_2 samples were prepared by using $La(NO_3)_3{\cdot}6H_2O$ (Merck, 99%), $Ce(NO_3)_3{\cdot}6H_2O$ (Aldrich, 99%), $Y(NO_3)_3$ (Aldrich, 99%), $Pr(NO_3)_3$ (Aldrich, 99%), $Sm(NO_3)_3$ (Aldrich, 99%), and TiO_2 (Degussa P25). The required amounts of the nitrate precursors were physically mixed with TiO_2 in a mortar and were calcined overnight in static air in a furnace at 600 or 800 °C, applying a heating rate of 10 °C/min. The target RE loading was 0.2, 1, or 2 wt%, respectively. For comparison, undoped P25 was heat-treated under the same conditions, and a series of La_2O_3, CeO_2, Y_2O_3, ZrO_2, PrO_2, and Sm_2O_3 was prepared by calcination of the nitrate precursors in the absence of TiO_2, also in similar conditions.

* Corresponding author.
E-mail address: g.mul@tudelft.nl (G. Mul).

0021-9517/$ – see front matter
doi:10.1016/j.jcat.2008.09.005

Doped samples are denoted as "P25_%RE_Temp," "%" being the target percentage of RE and "Temp" the calcination temperature. The undoped P25 photocatalysts are named P25_600 and P25_800.

2.2. Characterization

The Brunauer–Emmett–Teller (BET) surface area of the samples, was obtained by N_2 adsorption at −196 °C in a Quantachrome Autosorb 6B apparatus. Before the N_2 adsorption measurements, the samples were pretreated in vacuum at 110 °C for 16 h.

The X-ray diffraction (XRD) patterns were recorded on a Philips PW1840 X-ray diffractometer using Cu$K\alpha$ radiation at a scan rate of $2\theta = 0.01^\circ\,s^{-1}$ and used to identify the crystal phase and their corresponding crystallite size. The accelerating voltage and the applied current were 40 kV and 50 mA, respectively.

The relative abundance of anatase to rutile in the samples was calculated by using the following equation [11]:

$$F_r = \frac{1.26 I_r}{I_a + 1.26 I_r}, \tag{1}$$

where F_r is the rutile fraction, and I_r and I_a are the strongest intensities of the rutile (110) and anatase (101) diffraction angles, respectively.

The crystal sizes (D) of anatase and rutile were determined by employing the Scherrer equation:

$$D = \frac{K\lambda}{\beta \cos\theta}, \tag{2}$$

where λ is the wavelength of the Ni-filtered Cu$K\alpha$ radiation used ($\lambda = 0.15418$ nm), β the full width at half-maximum of the diffraction angle considered, K a shape factor (0.9) and θ the angle of diffraction. For these calculations the indices (101) for anatase and (110) for rutile were used.

The IR absorption spectra of the solid samples were recorded using a Thermo Nicolet Nexus spectrometer with a MCT detector and a Spectratech diffuse reflectance accessory equipped with a high temperature cell. The spectrum of KBr at 120 °C in flowing He (30 ml/min) was used as background. Water was removed from the catalyst surface to facilitate the analysis of the OH-group composition by recording the spectra at 120 °C after equilibration for 15 min in flowing He (25 ml/min), applying a ramp rate of 10 °C/min. All spectra were recorded from 4000–700 cm^{-1} by collecting 64 scans with a resolution of 4 cm^{-1}. The Kubelka–Munk (K–M) and reflectance–absorbance transformations were considered in evaluating the data. In a recent evaluation by Meunier et al. [12], it was determined for a comparable DRIFT accessory and transmission values below 60%, that the correlation between concentration of surface species and K–M band intensity was more linear than obtained by using the reflectance–absorbance intensity. After comparing the spectra of the TiO_2 samples in the present study, in conjunction with the deconvolution procedure, the K–M format gave the best results for the various samples. Hence spectra are represented in the K–M format throughout this study.

Steady-state fluorescence spectra were recorded on a Photon Technology International Photoluminescence setup. The catalysts were packed in a sample holder with a 67° angle towards the light of excitation. The samples were excited at 370 nm, close to the wavelength of the black-light used to activate the catalysts for methylene blue decomposition, as discussed below.

2.3. Photocatalytic tests

Methylene blue (MB) was obtained from Merck (97%) and used without further treatment. Photocatalytic activity measurements were carried out in a combinatorial screening assembly, outlined in Fig. 1. In each run up to 10 parallel experiments could be performed simultaneously. Preliminary photocatalytic experiments proved that all 10 reactors behaved identically and the results between runs were comparable within ±5% error range [13]. The UV irradiation was delivered by 8 blacklight lamps (18 W, Philips) maximizing at 370 nm, providing a light flux of 470 ± 20 μW/cm^2 entering the TiO_2/methylene blue suspension, as indicated in Fig. 1. For each experiment 50 mg of photocatalyst, sieved to a fraction of 53–75 μm, was added to a 100 ml aqueous solution of MB (0.03 mmol/l). Before the start of the reaction, the mixture was stirred using a magnetic stir-bar in the dark for 2 h to establish MB adsorption-equilibrium. During the reaction the reactor housing was continuously purged with a fan and the temperature was controlled at 32 ± 2 °C. Samples were withdrawn at constant time intervals and filtered through a 0.45 μm PTFE Millipore membrane filter to remove suspended catalyst agglomerates. Experimental checks proved that the amount of MB retained by the filter was negligible. Furthermore, reference experiments indicated that the photosensitized degradation of MB did not take place in the absence of photocatalysts. A UV–vis spectrometer was used to record the absorbance spectra of the solutions in the 400–1000 nm range with a spectral resolution of 0.33 nm. Calibrations were taken at 10 wavelengths adjacent to the maximum absorbance of MB at 667 nm. A Lambert–Beer diagram, typically in the form of absorbance

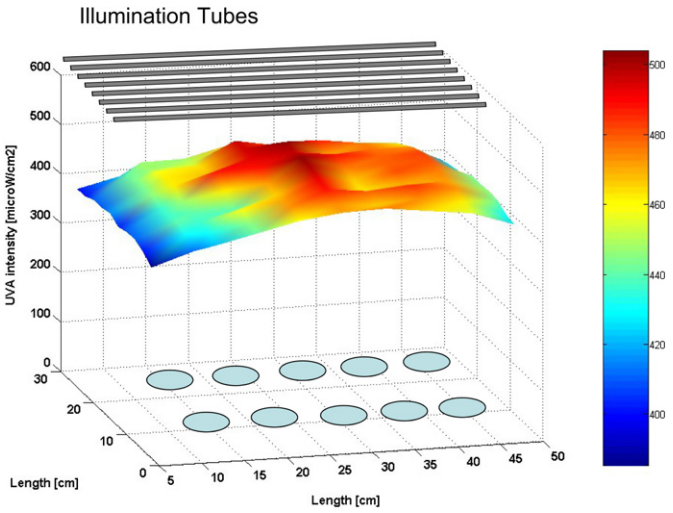

Fig. 1. Illustration of the applied photocatalytic setup. The dimensions of the box containing the reactors are shown, including the measured irradiance (μW/cm^2) at 370 nm at the height of the reactors containing the P-25 methylene blue slurries.

$$A = -\log(I/I_0) = \varepsilon bc \tag{3}$$

was established to correlate the absorbance to MB concentration, where ε is the wavelength-dependent molar absorption coefficient with units of $m^2\,mol^{-1}$, b is the light path length (m), and c is the MB concentration ($mol\,m^{-3}$).

3. Results

3.1. Textural analysis

The BET surface areas of the different samples are compiled in Table 1. It is well-known that P25 consists of non-porous nanoparticles [14]. The BET surface area of the TiO_2 photocatalyst P25 was 51 m^2/g, and little difference was observed in total surface area after calcination at 600 °C, both for P25_600, and all rare earth modified samples (P25_0.2RE_600). However, further increase of the thermal treatment temperature results in a significant reduction of surface area of un-promoted P25, to 16 m^2/g (P25_800).

Table 1
Characterization of samples

Sample	Anatase fraction[a] [nm]	Anatase crystal size[a] [nm]	Rutile crystal size[a] [nm]	Band gap energy [eV]	S_{BET} [m^2/g]
P25	0.70	22	37	3.25	51
P25_600	0.70	25	36	3.23	47
P25_0.2La_600	0.71	28	41	3.23	46
P25_0.2Ce_600	0.71	27	50	3.19	47
P25_0.2Y_600	0.72	28	39	3.16	46
P25_0.2Pr_600	0.71	27	50	3.14	47
P25_0.2Sm_600	0.70	26	47	3.16	46
P25_800	0.05	–	43	3.04	16
P25-0.2La-800	0.22	31	43	3.03	23
P25-0.2Ce-800	0.15	35	45	3.04	19
P25-0.2Y-800	0.13	30	50	3.02	20
P25-0.2Pr-800	0.31	35	47	3.02	24
P25-0.2Sm-800	0.08	29	50	3.01	17
P25-1La-800	0.31	35	45	3.05	25
P25-1Ce-800	0.48	31	47	3.07	30
P25-1Y-800	0.05	–	50	3.04	16
P25-1Pr-800	0.15	31	45	3.03	21
P25-1Sm-800	0.37	33	50	3.06	29
P25_2La_800	0.14	34	47		21
P25_2Ce_800	0.15	35	49		18

[a] Determined from XRD.

Comparison of this value with the remaining surface area of the 0.2 wt% RE-doped samples calcined at 800 °C shows that doping of P25 partially stabilizes the textural properties, resulting in surface areas in the range of 17–24 m^2/g. Enhancing the rare earth amount to 1 wt% showed an enhanced stabilization effect, with the BET area ranging from 16–30 m^2/g. Further enhancement of the RE-content to 2 wt% was detrimental.

3.2. X-ray diffraction

Based on the XRD characterization (not shown for brevity), both anatase and rutile are present in the commercial P25 sample [14]. Both the anatase to rutile ratio (70:30) and the crystallite sizes (22 nm for anatase and 37 nm for rutile) are in good agreement with results found by other authors [14].

Characteristic diffraction lines of La_2O_3, CeO_2, Y_2O_3, ZrO_2, PrO_2, and Sm_2O_3 were not detectable in RE-doped P25 up to 1 wt% loading. On the contrary, the diffractograms of P25_2La_800 and P25_2Ce_800 (not shown for brevity) contained characteristic lines at $2\theta \sim 39.8°$ and 28.7°, respectively, indicating the formation of segregated phases of La_2O_3 or CeO_2. The anatase fractions of the various samples, as determined by Eq. (1), are compiled in Table 1.

Thermal treatment at 600 °C did not change the composition of P25, nor did the dopants affect the relative phase composition. Regardless of the type of doping, the anatase fraction in the photocatalysts calcined at 600 °C was about 0.70. In contrast, thermal treatment at 800 °C did change the morphology of P25, converting anatase to rutile, the remaining anatase fraction in P25_800 being only 0.05. For the RE-doped samples calcined at 800 °C, significant inhibition of phase transformation from anatase to rutile was observed, in agreement with the data of Zhang [8]. Doping of P25 with 0.2% RE retarded rutile formation, the anatase fraction following the decreasing order Pr > La > Ce > Y > Sm.

The inhibiting effect in phase transformation of P25 becomes more dominant by enhancing the doping concentration to 1 wt% of La, Ce or Sm, while a higher amount is less effective for Y and Pr. An increase in the RE concentration to 2 wt% is less effective in the inhibition of phase transformation, as shown in Table 1 for the La- and Ce-doped samples.

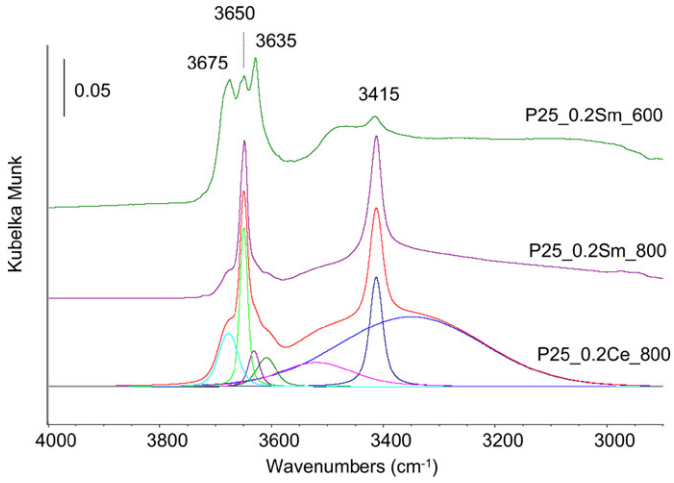

Fig. 2. DRIFT spectra for selected RE-doped P-25 catalysts. Top to bottom: P25_0.2Sm_600, P25_0.2Sm_800, and P25_0.2Ce_800. Spectra were recorded at 120 °C in 30 ml/min He. For P25_0.2Ce_800 the deconvoluted bands are also shown.

3.3. DRIFT characterization

The IR spectra of selected samples in the region of 4000–2800 cm^{-1}, where O–H stretching modes are expected, are shown in Fig. 2 after the K–M transformation. Upon heating fresh samples from room temperature up to 120 °C in He, the amount of adsorbed water on the surface of the catalysts decreases, allowing a better evaluation of the nature of the various OH-groups. The top-spectrum recorded at 120 °C (Sm-doped TiO_2, calcined at 600 °C) consists of 4 main contributions in the 3800–3600 cm^{-1} range [15–18]. The complicated spectral signature is the result of OH being present on different defect sites, as well as the result of contributions of both rutile and anatase phases [16]. The absorption at 3675 cm^{-1} is assigned to an isolated anatase vibration [16–18]. For the band at 3635 cm^{-1} we follow the assignment of Surca Vuk et al. [15], to anatase bridging $(Ti)_2$–OH [15]. The absorption bands for O–H stretching modes representing rutile are located at 3650 and at 3415 cm^{-1}, respectively [15–18]. For the band at 3415 cm^{-1} an assignment has been proposed to water molecules strongly adsorbed on TiO_2 (rutile) via interactions with coordinatively unsatured Ti^{4+} surface cations [17]. As expected on the basis of the XRD data, these bands contribute significantly to the spectra of the samples calcined at 800 °C, as illustrated by the spectra of Sm-doped TiO_2, and Ce-doped TiO_2, respectively.

Peak areas were calculated after deconvolution of a selected series of catalysts with the OMNIC™ program. The deconvoluted spectra for P25_0.2Ce_800 are also shown in Fig. 2. From the deconvoluted spectra, areas were determined for the contributions of rutile (3650, 3415 cm^{-1}), and anatase (3675, 3635 cm^{-1}) associated vibrations, respectively. While other contributions, centered at 3610, 3520, and 3350 cm^{-1}, were taken into account to obtain the best fit, these were considered to be related to remaining physisorbed water [17,18]. Unfortunately it was not possible to completely remove these water bands in the conditions of the measurements (flowing He, 120 °C). Consequent perturbations of the vibrational patterns and intensity of the hydroxyl groups, depending significantly on the relative location of adsorbed water molecules and type of hydroxyl group, do not allow a full quantitative analysis. Still, the calculated band areas for selected samples calcined at 800 °C are compiled in Fig. 3. For each sample, the first two bars represent the rutile contributions, and the last two bars the anatase contributions. While, as stated, the absolute values of the intensities should be considered semi-quantitative [12] in view of the water perturbations, generally it can be concluded that the number of anatase–OH groups is decreasing in the order La > Pr >

Ce > Sm, which is in good agreement with the decreasing anatase fraction in the samples as determined by XRD (Table 1).

The decreasing amount of anatase–OH is not compensated by an increasing contribution of rutile associated bands (Fig. 3). The intensity of rutile associated bands decreases in the series La > Ce > Sm ≫ Pr.

Applying 2 wt% doping, instead of 0.2 wt%, further decreases the amount of anatase–OH-groups (not shown for brevity). Most likely this is a result of more extensive surface coverage with RE, and the 20% reduction in surface area (compare Table 1).

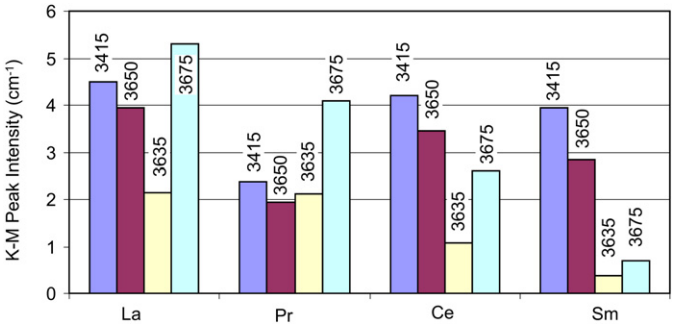

Fig. 3. Intensities of the various OH-vibrations for selected 0.2 wt% RE-doped TiO_2 samples, as determined after spectral deconvolution by the procedure illustrated in Fig. 2. The first two bars indicate the rutile contributions, the second two bars the anatase contributions of each RE (La, Pr, Ce, Sm).

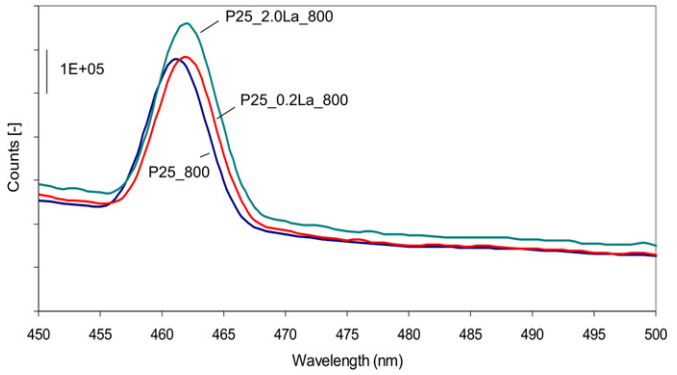

Fig. 4. Photoluminescence spectra of P25_800, P25_0.2La_800, and P25_2.0La_800. Emission was induced by exposing the samples to 375 nm radiation.

3.4. Opto-physical characterization

The photoluminescence (PL) spectrum of the applied P-25 is compared with the La-doped analogues (0.2, and 2.0 wt%) in Fig. 4. Luminescence is the result of excitation of the samples at 375 nm. The emission band maximizing at 462 nm has been reported previously [19], and is common for TiO_2 based materials. It is clear from Fig. 4 that the luminescence properties of P-25 are hardly affected by the incorporation of La in the sample. This clearly demonstrates that La^{3+} doping does not give rise to new PL phenomena, in agreement with literature data showing no effect of Sm doping [19].

3.5. Photocatalytic activity

Fig. 5 shows methylene blue degradation profiles for the La- and Ce-doped catalysts. Absorption of methylene blue on the catalyst surface (before $t = 0$) is only slightly affecting the total MB concentration in solution. The lines in Fig. 5 represent the fitted curves of a first order kinetic model in MB degradation by light exposure:

$$C_{MB} = C_{MB,0} e^{-k_{app} t} \quad (4)$$

in which C_{MB} and $C_{MB,0}$ are the MB concentrations at time (t), and ($t = 0$), respectively, and k_{app} the apparent first order rate constant. In all experiments first order kinetics is observed. Comparing the activity profiles in Fig. 5, the photocatalytic activity of P25 is affected by the RE, this effect depending on the nature of RE, the RE loading and the preparation temperature. For instance, profiles in Fig. 5a show that 0.2 and 1%-La loading improve the P25_800 photocatalytic activity, while increasing the La loading to 2 wt% slightly decreases the activity. Fig. 5b shows that P25_1.0Ce_800 yields the best activity among the 800 °C-calcined Ce-doped samples. Experiments performed with La_2O_3, CeO_2, Y_2O_3, PrO_2, and Sm_2O_3 showed that these oxides hardly degrade MB under the applied experimental conditions.

In Fig. 6, the kinetic rate constants of the 0.2% RE-doped photocatalysts calcined at 600 and 800 °C and the constants corresponding to P25_600 and P25_800 are compiled. The errors as determined from the 95% confidence interval of the apparent first order

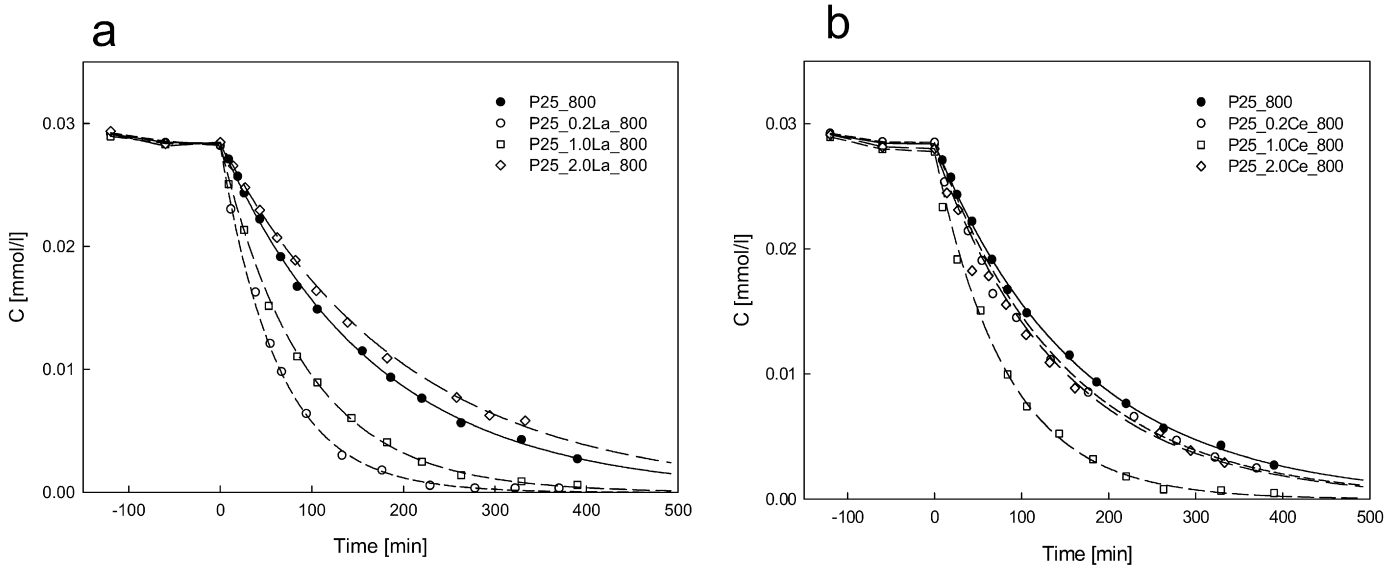

Fig. 5. Methylene blue photocatalytic degradation profiles for selected photocatalysts. (a) P25_%La_800, and (b) P25_%Ce_800.

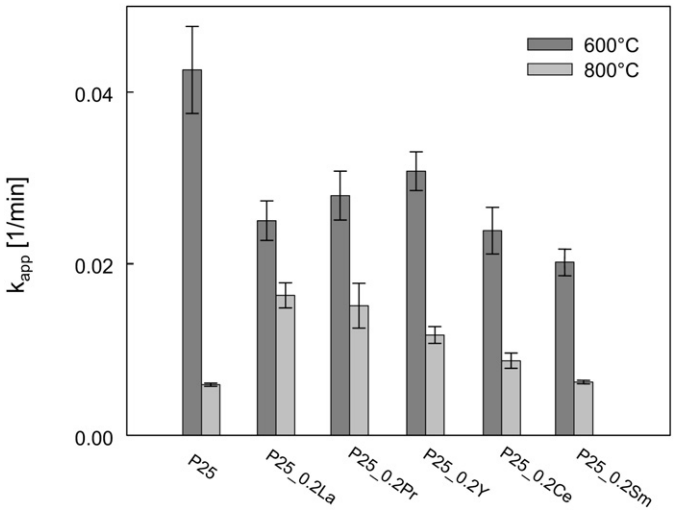

Fig. 6. Apparent first order rate constants as a function of RE amount and calcination temperature.

rate constant (Fig. 5) were lower than 10%. Comparing the apparent first order rate constants of P25_600 and P25_800, thermal treatment has a significant deteriorating effect on the photocatalytic activity. In case of the 600 °C-calcined samples, Fig. 6 indicates that all the RE-doped samples have lower photocatalytic activity than pure P25_600, the remaining activity depending on the applied RE. On the contrary, in case the photocatalysts were calcined at 800 °C, the photocatalytic activity of the RE-doped samples is higher than unpromoted P25_800, the performance again depending on the nature and loading of the RE. In particular La-, Y-, Pr-, and Ce-doped P-25 yield higher first-order rate constants in MB degradation than unpromoted P25_800, whereas for Sm the positive effect is less dramatic. Without presenting all the details, increasing the loading of RE above 0.2 wt% generally does not improve the performance of P25_800. The decrease in activity of the samples calcined at 800 °C is in good agreement with the decreasing contribution of anatase–OH in the DRIFT spectra (compare Fig. 3), as will be discussed in the following.

4. Discussion

As was stated in the introduction the aim of the present study was to contribute to the evaluation of the effect of lanthanides and high temperature treatment on the photocatalytic activity of TiO_2 in methylene blue degradation, by monitoring changes in phase composition, surface area, and surface hydroxyl-group composition of P-25. In the following the effect of these parameters on the photocatalytic activity will be discussed.

4.1. Activity of rare earth oxides

Pure rare earth oxides have very little activity in photocatalytic methylene-blue decomposition, in agreement with the reported low activity in salicylic acid decomposition reported by Ranjit et al. [9,10]. This is in agreement with the absence of absorption bands at the wavelength of the light emitted (370 nm) by the 'black-light' sources, used to stimulate methylene blue decomposition. Hence, activity differences are most likely the result of (surface) structural changes of TiO_2, induced by the applied thermal treatments in the presence or absence of the dopants, rather than reaction of methylene blue over RE-sites.

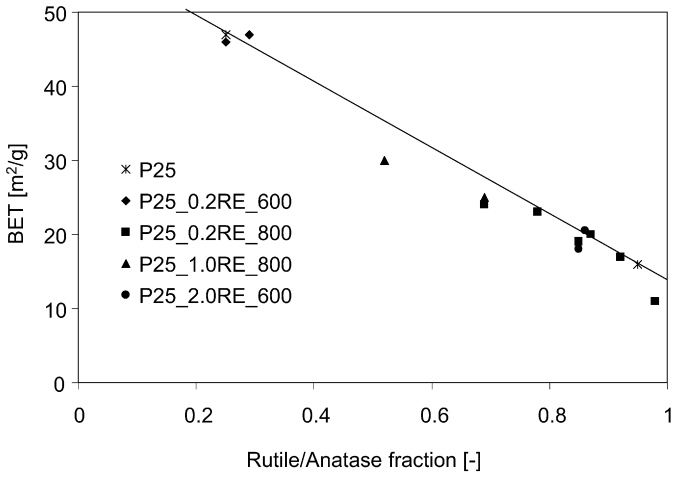

Fig. 7. Correlation between the rutile/anatase fraction and BET area of the various photocatalysts. Legend as indicated in the figure.

4.2. Phase composition and surface area

When pure P25 is heated to 800 °C, the content of rutile, which is the thermodynamically favored phase, increases from 30 to 95%, as was deduced both from XRD, and DRIFT characterization. The anatase to rutile phase transformation is generally considered to be a nucleation and growth process during which rutile nuclei form within the anatase phase [14,20,21]. Clearly the rutile phase has a significantly lower activity than the mixed rutile/anatase composition of P-25_600. The data in Table 1 show that the phase transformation is largely prevented by doping, as previously reported in [14,22]. This is a result of the formation of tetrahedral Ti species, whose interaction with octahedral Ti sites in anatase is thought to prevent the phase transformation to rutile [20–22]. It should be mentioned that a direct correlation between the anatase fraction of 4 selected photocatalysts, containing 0.2 wt% Ce, Pr, La, and Sm, and the photocatalytic activity was not obtained. In agreement with the statements of Ranjit et al., significant differences in photocatalytic activity can apparently not be attributed to the differences in phase composition alone [9,10]. Further, a treatment at 800 °C might produce novel dopant/TiO_2 interactions that a treatment of the doped materials limited to 600 °C does not induce. However, measurements (Fig. 4) indicate that the photoluminescence properties are not largely affected by the rare earth ions and/or variations in calcination temperature, in agreement with the literature [19]. Although it is not straight forward to correlate photoluminescence properties to photocatalytic activity, the photoluminescence data suggest that changes in the opto-physical properties are minor, and not an explanation for the observed differences in photocatalytic activity.

From the library of catalysts, a correlation can be deduced describing the surface area as a function of the anatase fraction. This linear correlation is shown in Fig. 7. Based on this correlation, it is obvious that the phase composition and the surface area are coupled. This correlation indicates that the different statements on the effect of the anatase to rutile ratio on photocatalytic activity made in the literature, at least for P-25 modified by heat treatment, cannot be discussed independently from an effect of the available surface area. Since we did not find a good correlation between the anatase fraction and the first order kinetic rate constant of methylene blue decomposition, as expected a good correlation between the first order kinetic rate constant and the BET area was not obtained. Another factor must play an important role in determining catalytic activity [9,10].

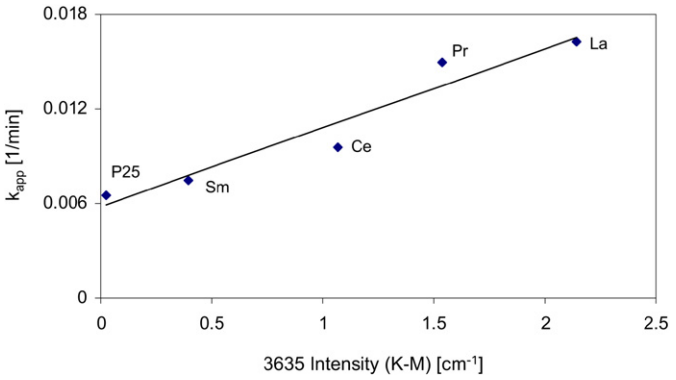

Fig. 8. Correlation between the apparent first order rate constants of the various photocatalysts, and the corresponding intensity of the 3635 cm^{-1} band, obtained after spectral deconvolution of the K–M representation. Legend as indicated in the figure for the catalysts calcined at 800 °C.

4.3. Surface hydroxyl groups

Photostimulation of TiO_2 generates electrons and holes, and (hydrated) Ti^{4+}–OH entities on the surface trap the hole by formation of surface hydroxyl radicals (Ti^{4+}–OH•) [23]. It has been proposed that the first step in the oxidation of organic compounds is the reaction of these (surface) OH• radicals with the organic molecule. The deconvoluted DRIFT data allow us to distinguish between the various surface OH-groups. Plotting the first order kinetic rate constant of MB decomposition against the sum of intensities of all IR bands, or the rutile associated IR bands, does not give a good correlation. On the contrary, the amount of anatase hydroxyl-groups shows a good correlation with the degradation rate of MB, and in particular the quantity of the bridging $(Ti)_2$–OH (3635 cm^{-1}), as illustrated in Fig. 8. It should be noticed, however, that the trendline in Fig. 8 does not go through the origin, suggesting that other (hydrated) TiO_2 sites also contribute to photocatalytic activity.

The photocatalytic tests were carried out on TiO_2 materials suspended in an aqueous medium. The $(Ti)_2$–OH (3635 cm^{-1}) site observed in the DRIFT spectra of the partially dehydrated systems should therefore be considered as a precursor for the actual site during the reaction, which is largely altered by the extensive water population on the catalyst surfaces in aqueous conditions. It is to be assumed that this site has the highest efficiency in trapping the photo-generated holes by formation of surface hydroxyl radicals (Ti^{4+}–OH•) [23]. Unfortunately, the exact nature of the active site will be extremely difficult to assess by IR spectroscopy, even if the ATR technique is applied, in view of the large and broad spectral contribution of water, overlapping the OH-vibrations.

The questions remaining are (i) why the different RE dopants affect the remaining anatase fraction and (partially dehydrated) hydroxyl group intensity differently (by calcination at 800 °C), and (ii) why the hydroxyl group intensity does not change linearly with a change in anatase fraction (compare Table 1 and Fig. 8). The answer to both questions is related to the temperature and rate at which the RE nitrate precursor decomposes, which determines to what extent the RE-oxide becomes dispersed over the TiO_2 surface. Clearly, the dispersion of the RE-oxide will in turn determine the extent of the anatase to rutile conversion at 800 °C, as well as the amount of remaining surface exposed Ti–OH groups, not necessarily to the same degree. Changing the catalyst preparation procedure (a.o. ramp rate, flow vs static conditions) might thus dramatically affect the outcome of the results presented in this study.

Summarizing, rather than a beneficial effect by retarding electron-hole recombination, or RE-assisted adsorption of MB, which should have led to better performance of our RE-doped P25 samples pretreated at 600 °C, we propose that the positive effect of the addition of RE after treatment at 800 °C, at least in the methylene blue decomposition reaction, is the result of a stabilizing effect on the amount of remaining anatase $(Ti)_2$–OH-groups, which is in turn affected by the extent of dispersion of the RE-oxide. As was recently shown by Ryu and Choi, other properties of TiO_2 might be more important in controlling reactivity towards other substrates [24], which will be evaluated in future studies in our laboratory.

5. Conclusions

- Doping of P25 with rare earth oxides such as La, Ce, Y, Pr, and Sm prevents the anatase to rutile phase transformation upon calcination at 800 °C, positively affecting the remaining BET surface area. A linear correlation was found between the BET surface area and the anatase/rutile ratio in P25.
- The photocatalytic degradation of methylene blue over rare earth oxide modified TiO_2, follows first order kinetics, and is mainly dependent on the quantity of a specific anatase–OH group. This quantity is a function of the BET surface area (and hence anatase/rutile ratio) of the photocatalysts, and the quantity and extent of dispersion of the rare earth oxide.

Acknowledgments

The authors gratefully acknowledge the financial support by the Dutch Technology Foundation STW (Projects DPC 5772, and DPC 5551) and the Spanish MEC for the fellowship of ABL. Ir. M. Damen is acknowledged for performing the deconvolution procedure of the K_M formatted spectra.

References

[1] O. Carp, C.L. Huisman, A. Reller, Prog. Solid State Chem. 32 (2004) 33.
[2] O. Legrini, E. Oliveros, A.M. Braun, Chem. Rev. 93 (1993) 671.
[3] A. Mills, S. Le Hunte, J. Photochem. Photobiol. A 108 (1997) 1.
[4] S. Devahasdin, C. Fan, K. Li, D.H. Chen, J. Photochem. Photobiol. A 156 (2003) 161.
[5] L. Gao, H. Liu, J. Sun, Mat. Sci. Forum 486–487 (2005) 53.
[6] A.-W. Xu, Y. Gao, H.-Q. Liu, J. Catal. 207 (2002) 151.
[7] F.B. Li, X.Z. Li, M.F. Hou, Appl. Catal. B 48 (2004) 185.
[8] Y. Zhang, H. Xu, Y. Xu, H. Zhang, Y. Wang, J. Photochem. Photobiol. A 170 (2005) 279.
[9] K.T. Ranjit, I. Willner, S.H. Bossmann, A.M. Braun, J. Catal. 204 (2001) 305.
[10] K.T. Ranjit, I. Willner, S.H. Bossmann, A.M. Braun, Environ. Sci. Technol. 35 (2001) 1544.
[11] G. Cerrato, L. Marchese, C. Morterra, Appl. Surf. Sci. 70/71 (1993) 200.
[12] J. Sirita, S. Phanichphant, F.C. Meunier, Anal. Chem. 79 (2007) 3912.
[13] P. Du, H. Shibata, G. Mul, J.A. Moulijn, in: D. Ollis, H. Al-Ekabi (Eds.), Proceedings of the TiO_2-9/AOT-10 Conference, Univ. of West Ontario Press, San Diego, USA, 2005.
[14] A.K. Datye, G. Riegel, J.R. Bolton, M. Huang, M.R. Prairie, J. Solid State Chem. 115 (1995) 236.
[15] A. Surca Vuk, R. Jese, M. Gaberscek, B. Orel, G. Drazic, Sol. Energy Mater. Sol. Cells 90 (2006) 452.
[16] G. Martra, Appl. Catal. A 200 (2000) 275.
[17] C. Morterra, J. Chem. Soc. Faraday Trans. 84 (1988) 1617.
[18] G. Mul, A. Zwijnenburg, B. van der Linden, M. Makkee, J.A. Moulijn, J. Catal. 201 (2001) 128.
[19] Q. Xiao, Z. Si, J. Zhang, C. Xiao, Z. Yu, G. Qiu, J. Mater. Sci. 42 (2007) 9194.
[20] S. Hishita, I. Mutoh, K. Koumoto, H. Yanagida, Ceram. Int. 9 (1983) 61.
[21] J. Nair, P. Nair, F. Mizukami, Y. Oosawa, T. Okubo, Mater. Res. Bull. 34 (1999) 1275.
[22] Y.H. Zhang, H.X. Zhang, Y.X. Xu, Y.G. Wang, J. Solid State Chem. 177 (2004) 3490.
[23] A. Houas, H. Lachheb, M. Ksibi, E. Elaloui, C. Guillard, J.M. Herrmann, Appl. Catal. B 31 (2001) 145.
[24] J. Ryu, W.Y. Choi, Environ. Sci. Technol. 42 (2008) 294.